Catalysis Science & Technology

Accepted Manuscript

ROYAL SOCIETY OF CHEMISTRY

www.rsc.org/catalysis

Ozone catalytic oxidation for ammonia removal from simulated air at room temperature

Yang Liu[a], Xiao-Song Li[a], Jing-Lin Liu[a], Chuan Shi[a], Xiaobing Zhu[a,*], Ai-Min Zhu[a], Ben W.-L. Jang[b,*]

[a]*Laboratory of Plasma Physical Chemistry, Dalian University of Technology, 116024 Dalian, China*

[b]*Department of Chemistry, Texas A&M University-Commerce, PO Box 3011, Commerce, TX 75429, United States*

---

* Corresponding authors. Fax: +86-411-84706094 (X. Zhu), +1-903-468-6020 (B.W.-L. Jang).
E-mail addresses: xzhu@dlut.edu.cn (X. Zhu), Ben.Jang@tamuc.edu (B.W.-L. Jang).

ABSTRACT

Ozone catalytic oxidation (OZCO) for removing ammonia from simulated air over AgMn/HZSM-5 (AgMn/HZ) catalyst with high ammonia conversion and high N_2 selectivity at room temperature is reported for the first time. HZ, Ag/HZ, Mn/HZ and AgMn/HZ catalysts were compared in the OZCO reactions of gaseous and adsorbed NH_3. In OZCO of gaseous NH_3, N_2 was the major product and N_2O was the minor product. NH_3 conversion dropped quickly with time-on-stream (TOS) over HZ and Ag/HZ catalysts while it remained almost constant at a high level over Mn/HZ and AgMn/HZ catalysts during the entire test. N_2 selectivity of AgMn/HZ catalyst was higher than that of Mn/HZ catalyst. When the initial concentration of NH_3 was 521 ppmv and the ratio of initial concentration of O_3 to NH_3 was 1.73, 99% of NH_3 conversion with 94% of N_2 selectivity was obtained over AgMn/HZ catalyst at room

temperature and 150,000 $ml \cdot g^{-1} \cdot h^{-1}$ of gas hourly space velocity (GHSV). Finally, the pathways for OZCO of NH_3 were proposed for the four catalysts based on the comparative investigation of the gaseous products and surface species during OZCO of adsorbed and gaseous NH_3.

Keywords: Catalytic oxidation; Ozone; Ammonia removal; AgMn/HZSM-5 catalyst.

1. Introduction

Ammonia, which is a toxic, corrosive and reactive gas with an irritating odor, is considered as a highly hazardous pollutant and of great importance in PM 2.5 formation and acid rain deposition.[1] Due to the increasing environmental concerns, NH_3 removal from air is becoming a serious issue. Selective catalytic oxidation (SCO) of NH_3 to N_2 is an ideal technology for NH_3 abatement.[2-12] Several catalysts have been proposed for SCO of NH_3, however, they usually require high temperatures and, therefore, are energy-consuming. Typically, Pt or PtO based catalysts, supported on γ-Al_2O_3 or HZSM-5 (HZ) zeolites, required temperatures of 200-250 ℃ to achieve 100% of NH_3 conversion using O_2 (gas hourly space velocity (GHSV[‡]) = 60,000 $ml{\cdot}g^{-1}{\cdot}h^{-1}$ with 1000 ppmv of NH_3).[2] Long *et al.*[5] have prepared several Fe based catalysts, such as Fe_2O_3-TiO_2, Fe_2O_3-ZrO_2, Fe_2O_3-Al_2O_3 and Fe_2O_3-SiO_2, for SCO of NH_3 and found that 95-99% of NH_3 conversion could be obtained at temperatures as high as 500 ℃ (GHSV = 150,000 $ml{\cdot}g^{-1}{\cdot}h^{-1}$ with 1000 ppmv of NH_3). Lippits *et al.*[10] and Liang *et al.*[12] reported that, over Cu/γ-Al_2O_3 catalysts, 100% of NH_3 conversion was achieved at temperatures exceeding 300 ℃ (GHSV = 12,000 $ml{\cdot}g^{-1}{\cdot}h^{-1}$ with 20,000 ppmv of NH_3[10] and 30,000 $ml{\cdot}g^{-1}{\cdot}h^{-1}$ with 1000 ppmv of NH_3,[12] respectively).

O_3, which is a strong oxidant, has attracted extensive attention and is now being widely investigated in the catalytic removal of toxic substances from polluted gases because its performance in such reactions is superior to that of O_2. On the basis of the results from Mehandjiev and co-authors,[13-16] using O_3 instead of O_2 permitted the reaction to proceed in a low-temperature range and achieved a high catalytic activity.

The data obtained using manganese oxide as the catalyst demonstrated that the activation energy in catalytic benzene oxidation using O_3 was three times lower than that using O_2.[13] O_3 has been frequently used for the removal of benzene,[13,17-26] toluene,[27-33] chlorobenzene,[34,35] formaldehyde[36,37] and carbon monoxide,[14,16,38-40] *etc*. However, to the best of our knowledge, very few studies focused on the ozone catalytic oxidation (OZCO) of NH_3. One is reported by Kastner and co-authors,[1] who investigated OZCO of NH_3 at room temperature using wood fly ash and biomass char as catalysts. However, the best NH_3 conversion achieved was around 60% at relatively low GHSV of 76,200 $ml \cdot g^{-1} \cdot h^{-1}$ and low inlet NH_3 concentration of about 11 ppmv. Another is reported by Ichikawa *et al.*,[41] but it is about aqueous-phase reaction of NH_4^+ with O_3.

Manganese oxide catalysts are highly active for ozone decomposition[13,17,25,27,42] and the supported Ag catalysts were reported to be active for NH_3 oxidation.[6] HZ zeolites are often used as catalyst supports in NH_3 oxidation processes, since the acid sites in HZ can enhance the adsorption and activation of NH_3 molecules and the pore structure of HZ favors NH_3 oxidation to N_2.[4,7] Herein, the investigation on OZCO of NH_3 over the well-defined HZ supported Ag and/or Mn catalysts is reported in this study. To clarify the reaction mechanisms for OZCO of NH_3, OZCO of adsorbed NH_3 is also examined comparatively over the same catalysts.

2. Experimental

2.1. Catalyst preparation

HZ-supported catalysts were prepared via incipient wetness impregnation method using HZ (SiO_2/Al_2O_3 = 360, BET‡ surface area = 341 $m^2 \cdot g^{-1}$, Catalyst Plant of Nankai University, China) as the support. $AgNO_3$ and $Mn(CH_3COO)_2 \cdot 4H_2O$ were used as Ag and Mn precursors, respectively. The impregnated samples were aged overnight at ambient temperature in darkness followed by drying at 110 ℃ for 6 h and calcination in static air in an oven at 450 ℃ for 3 h. The obtained powders were grounded, tableted, crushed and sieved to 20-40 mesh.

2.2. ICP & BET characterization and the chemical states of Ag and Mn species

Inductively coupled plasma-atomic emission spectroscopy (ICP-AES, optima 2000DV, USA) was used to determine Ag and Mn loadings. The Ag loading of Ag/HZ catalyst was 0.7 wt% and the Mn loading of Mn/HZ catalyst was 2.3 wt%. The Ag and Mn loadings of AgMn/HZ catalyst were 0.8 wt% and 2.4 wt%, respectively. The reason why the Ag loading of 0.8 wt% and Mn loading of 2.4 wt% were chosen for AgMn/HZ catalyst is based on our previous study,[26] which showed such AgMn/HZ catalyst possessing the best activity and stability in benzene oxidation by O_3.

The specific surface areas of the supported catalysts were measured by the N_2 adsorption BET method at -196 ℃ (Autosorb-1, Quantachrome, USA). The BET surface areas were 341, 334 and 336 $m^2 \cdot g^{-1}$ for Ag/HZ, Mn/HZ and AgMn/HZ catalysts, respectively.

As revealed by the XPS[25] and UV-vis Diffuse Reflectance Spectra[26] of the catalysts, Ag was present in metallic state over Ag/HZ and AgMn/HZ catalysts and Mn existed as a mixture of Mn^{3+} and Mn^{4+} over Mn/HZ and AgMn/HZ catalysts after

calcination.

2.3. Quantification methods of the concentrations of NH_3, N_2O, O_3, NO, NO_2 and N_2

For the quantification of NH_3, N_2O and O_3, the standard curves of "Strongest FT-IR peak height versus Concentration" were established on a Fourier transform-infrared (FT-IR) spectrometer (Nicolet-Antaris IGS Analyzer, Thermo, USA). For the standard curves of NH_3 and N_2O, their concentrations were given by their standard gases. For O_3 standard curve, due to O_3 standard gas being unavailable, O_3 concentrations were calibrated by the iodometric titration method. The strongest peak heights at 1000-900 cm^{-1}, 2300-2150 cm^{-1} and 2150-2000 cm^{-1} were used for the quantification of NH_3, N_2O and O_3, respectively.

However, for NO (2000-1800 cm^{-1}) and NO_2 (1700-1500 cm^{-1}), their concentrations could not be precisely evaluated by the FT-IR spectrometer alone due to the superposition of H_2O (2000-1200 cm^{-1}). Therefore, NO and NO_2 were quantified with mass spectrometer (HPR 20 QIC, HIDEN Analytical, England) by the internal standard method. The product of N_2O was used as the internal standard because its concentration could be determined simultaneously by the FT-IR spectrometer. The specific quantification methods of NO, NO_2 and N_2 are described in Supplementary Data.

2.4. OZCO of gaseous NH_3 and investigation of the surface species after OZCO process

Catalytic reactions were carried out with a fixed-bed flow reactor. A quartz

U-tube reactor (i.d. 4 mm) with about 0.1 g of catalyst was immersed in water bath at 17 ℃. Ozone was generated from pure O_2 (purity ＞ 99.999%) by a homemade ozone generator and monitored online by the FT-IR spectrometer. Before performing the experiments, all catalysts were pretreated in a dry simulated air stream at 450 ℃ for 1 h and then cooled down to room temperature in the same atmosphere. The feed gas of 250 SCCM‡(Standard Cubic Centimeters per Minute), containing NH_3, O_3, 20 vol.% of O_2 and balanced by N_2, was flowed through the catalyst bed, which corresponded to a GHSV of 150,000 $ml \cdot g^{-1} \cdot h^{-1}$. Unless otherwise stated, NH_3 and O_3 concentrations were *c.a.* 530 ppmv and 450 ppmv, respectively. NH_3 conversion (X_{NH_3}), O_3 conversion (X_{O_3}), ratio of converted O_3 to NH_3 ($n_{O_3}^{Conv.}/n_{NH_3}^{Conv.}$), N_2O selectivity (S_{N_2O}) and N_2 selectivity (S_{N_2}) were calculated as follows:

$$X_{NH_3}(\%) = \frac{C_{NH_3}^{in} - C_{NH_3}^{out}}{C_{NH_3}^{in}} \times 100\% \quad (1)$$

$$X_{O_3}(\%) = \frac{C_{O_3}^{in} - C_{O_3}^{out}}{C_{O_3}^{in}} \times 100\% \quad (2)$$

$$n_{O_3}^{Conv.}/n_{NH_3}^{Conv.} = \frac{C_{O_3}^{in} \cdot X_{O_3}}{C_{NH_3}^{in} \cdot X_{NH_3}} \quad (3)$$

$$S_{N_2O}(\%) = \frac{C_{N_2O} \times 2}{C_{NH_3}^{in} \cdot X_{NH_3}} \times 100\% \quad (4)$$

$$S_{N_2}(\%) = 1 - S_{N_2O} \quad (5)$$

where $C_{NH_3}^{in}$ and $C_{NH_3}^{out}$ are the inlet and outlet NH_3 concentrations in the gas stream during OZCO of gaseous NH_3, respectively; $C_{O_3}^{in}$ and $C_{O_3}^{out}$ are the inlet and outlet O_3 concentrations in the gas stream during OZCO of NH_3, respectively; C_{N_2O} is the outlet N_2O concentration in the gas stream during OZCO of NH_3.

To verify the reliability of N_2 selectivity derived from eqn. (5), additional experiments using Ar as the balanced gas for direct measurement of N_2 were carried out: 0.2 g of AgMn/HZ catalyst, 500 SCCM of total flow rate with 1000 ppmv of NH_3 and 500 ppmv of O_3, 20 vol.% of O_2 and Ar balanced. The results are shown in Fig. S1. The N_2 selectivity in Fig. S1e was derived from the direct measurement according to eqn. (6):

$$S_{N_2}(\%) = \frac{C_{N_2} \times 2}{C^{in}_{NH_3} \cdot X_{NH_3}} \times 100\% \quad (6)$$

where C_{N_2} is the outlet N_2 concentration in the gas stream during OZCO of NH_3 and could be obtained from eqn. S(16). And the N_2 selectivities derived from eqns. (5) and (6) were 80% and *c.a.*75%, respectively. This confirms that the N_2 selectivity derived from eqn. (5) is reliable in this work.

After OZCO of NH_3, the used catalyst pellets were unloaded from the reactor, ground into powders for ATR (attenuated total reflectance) measurements and temperature programmed desorption (TPD) studies.

The ATR spectra were recorded on a Nicolet 6700 spectrometer (Thermo, USA) with an MCT detector (Mercury Cadmium Telluride detector, which needs to be cooled with liquid nitrogen). The catalyst powder was loaded onto the Smart ATR accessory with diamond as the ATR material. The background spectrum was recorded with the bare diamond and it was subtracted from the spectra of HZ, Mn/HZ, Ag/HZ and AgMn/HZ catalysts. The beam path inside the spectrometer was purged with purified CO_2-free dry air. The spectra were recorded by averaging 32 scans at a resolution of 4 cm^{-1}.

For the TPD experiments of the used catalysts, a helium stream was flowed through the catalyst bed of 0.03 g at a flow rate of 100 SCCM for 1 h until the baseline of the mass spectrometer became stable. The temperature was raised linearly at 10 ℃·min^{-1} to 450 ℃ and held for 30 min afterwards.

2.5. OZCO of adsorbed NH_3

2.5.1. Investigation of surface adsorption sites on the catalysts towards NH_3 by NH_3-TPD

NH_3-TPD tests were carried out with 0.1 g of catalyst under an Ar stream of 100 SCCM. Before the TPD measurements, the samples were pretreated in 100 SCCM of Ar flow at 450 ^{o}C for 1 h and then cooled down to room temperature in the same atmosphere. The samples were then treated with 540 ppmv of NH_3 for 25 min. After that, the NH_3 stream was replaced with 100 SCCM of Ar flow for 1 h to remove the physisorbed NH_3. Subsequently, the temperature was increased in an Ar stream of 100 SCCM to 450 ^{o}C with a ramp of 10 ℃·min^{-1}.

2.5.2. OZCO of adsorbed NH_3 and investigation of the surface species after OZCO

After pretreated in dry simulated air at 450 ℃ for 1h and cooled down to room temperature, the samples were treated with 540 ppmv of NH_3 for 25 min at room temperature. Then the NH_3 stream was replaced with 250 SCCM of He flow containing 20 vol.% of O_2 for 40 min to remove the physisorbed NH_3. After that, a feed gas of 250 SCCM, containing 450 ppmv of O_3, 20 vol.% of O_2 and balanced by He, was flowed through the catalyst bed for 30 min. In order to present how much

N_2O was produced during OZCO of adsorbed NH_3, $N_2O/(N_2+N_2O)$ was defined as follows:

$$N_2O/(N_2+N_2O)(\%) = \frac{F\cdot\int_0^t C_{N_2O}\cdot dt}{F\cdot\left(\int_0^t C_{N_2}\cdot dt + \int_0^t C_{N_2O}\cdot dt\right)}\times 100\% \quad (7)$$

where F and t are the total flow rate and oxidation time during OZCO of adsorbed NH_3, respectively. And the integral is the area under the curve for N_2 or N_2O versus time during OZCO of adsorbed NH_3.

Thereafter, ATR and TPD experiments were performed over the used catalysts under the conditions described in **Section 2.4.**

3. Results and discussion

3.1. OZCO of gaseous NH_3

3.1.1. Comparison of OZCO of gaseous NH_3 over HZ, Mn/HZ, Ag/HZ and AgMn/HZ catalysts

Based on the results of Olszyna *et al.*,[43] mixtures of NH_3 and O_3 could react at 30 ℃ in gaseous phase. Therefore, a control consisting of a reactor system without catalyst was operated at room temperature, 250 SCCM of dry simulated air with 527 ppmv of NH_3 and 446 ppmv of O_3. The result shows that almost no NH_3 conversion was observed, which demonstrates that the gaseous reaction of O_3 and NH_3 could be neglected in this study.

The catalytic performance of HZ and HZ-supported catalysts was evaluated in the OZCO of gaseous NH_3 and the results are presented in Fig. 1. Fig. 1a shows the

variation of NH_3 conversion with time-on-stream (TOS) during NH_3 oxidation using O_3. As shown in Fig. 1a, Ag/HZ and Mn/HZ catalysts possessed much higher NH_3 conversion than the bare HZ support did, which indicates that the addition of Ag or MnO_x greatly enhanced the NH_3 oxidation. Compared with the Mn/HZ catalyst, the increase of NH_3 conversion on AgMn/HZ catalyst was not significant, since Mn/HZ catalyst had already possessed very high NH_3 conversion before the addition of Ag.

In terms of catalyst stability, NH_3 conversion dropped quickly with TOS over HZ and Ag/HZ catalysts. However, the conversion was almost constant around 50% over Mn/HZ and AgMn/HZ catalysts during the entire reaction. The results demonstrate that the addition of MnO_x greatly suppressed catalyst deactivation and enhanced the catalyst stability.

Additionally, as shown in Fig. 1b, O_3 conversion remained relatively constant at 60% and 80% over HZ and Ag/HZ catalysts, respectively. The relatively constant conversion of O_3 with decreasing conversion of NH_3 suggests that the usage of O_3 for NH_3 oxidation decreases with time over HZ and Ag/HZ. However, for Mn/HZ and AgMn/HZ catalysts, O_3 conversion was at 100% during the entire test. This should be ascribed to the very high activity of manganese oxides on O_3 decomposition and the consistent usage of O_3 for NH_3 oxidation throughout the test.[13,17,25,27,42]

In all four cases, N_2 was the main gaseous product with small amount of N_2O. NO or NO_2 was not detected during OZCO of gaseous NH_3. As shown in Fig. 1c, N_2O and N_2 selectivities of the catalysts were compared among all four catalysts. In general, the N_2 selectivities were high on all samples, exceeding 80%. However,

Ag/HZ catalyst possessed the highest N_2 selectivity of 95% while Mn/HZ catalyst was the least selective to N_2 among all catalysts. The oxidation of NH_3 can be described as the abstraction of hydrogen process,[44] in which the H atoms in the NH_3 molecules were abstracted one by one to form adsorbed NH_x species and N atoms. Then the N atoms could either be further oxidized into NO, which can react with NH_x to form N_2, or further react with NO formed and release as N_2O.[44] The reason why that the N_2 selectivities over HZ and Ag/HZ catalysts were slightly higher than those of Mn/HZ and AgMn/HZ catalysts (Fig. 1c) is not clear at this point. Since the N_2 selectivity of AgMn/HZ catalyst (about 87%) was higher than that of Mn/HZ catalyst (*c.a.* 80%) (Fig. 1c), it indicates that Ag is beneficial to promote the selective oxidation of NH_3 to N_2 during OZCO of gaseous NH_3.

The $n_{O_3}^{Conv.}/n_{NH_3}^{Conv.}$ ratio during NH_3 oxidation is summarized in Fig. 1d. As shown in Fig. 1d, the $n_{O_3}^{Conv.}/n_{NH_3}^{Conv.}$ ratio was relatively constant around 1.7 over Mn/HZ and AgMn/HZ catalysts during the entire reaction. However, for HZ and Ag/HZ catalysts, their $n_{O_3}^{Conv.}/n_{NH_3}^{Conv.}$ ratios were low at the beginning of OZCO reaction and then increased fast with TOS, especially for HZ, the $n_{O_3}^{Conv.}/n_{NH_3}^{Conv.}$ ratio of which arrived at about 2 at TOS = 60 min. Again, these results suggest that Mn/HZ and AgMn/HZ are more efficient and stable in O_3 utilization for NH_3 oxidation.

3.1.2. Effects of $C_{O_3}^{in}/C_{NH_3}^{in}$ ratio over AgMn/HZ catalyst

Fig. 2 shows the effects of $C_{O_3}^{in}/C_{NH_3}^{in}$ ratio on the NH_3 oxidation by O_3 over AgMn/HZ catalyst at TOS = 60 min. Based on the proposed O_3 decomposition mechanism by Oyama and co-workers,[45] it is assumed that only one oxygen atom

derived from O_3 molecule is responsible for NH_3 oxidation. The production of N_2 and N_2O could be written as eqns. (8) and (9), respectively:

$$1.5\,O_3 + NH_3 \rightarrow 0.5\,N_2 + 1.5\,O_2 + 1.5\,H_2O \quad (8)$$

$$2\,O_3 + NH_3 \rightarrow 0.5\,N_2O + 2\,O_2 + 1.5\,H_2O \quad (9)$$

It can be seen from eqn. (8) that the stoichiometric ratio of O_3 to NH_3 is 1.5 for OZCO of NH_3 to N_2. When the $C^{in}_{O_3} / C^{in}_{NH_3}$ ratio was 0.85, which is about half of the stoichiometry, close to half of the NH_3 feed was excessive with respect to O_3. Therefore, the NH_3 and O_3 conversions are 51% and 100% at $C^{in}_{O_3} / C^{in}_{NH_3}$ = 0.85, respectively, as shown in Fig. 2. As the $C^{in}_{O_3} / C^{in}_{NH_3}$ ratio increased to 1.32, which is slightly lower than the stoichiometric ratio of 1.5, the NH_3 conversion rose to 84% and nearly all the O_3 was consumed (O_3 conversion was 95%, as shown in Fig. 2). Moreover, almost 100% of NH_3 conversion could be achieved at $C^{in}_{O_3} / C^{in}_{NH_3}$ = 1.73, which is slightly higher than the stoichiometric ratio of 1.5. In this case, O_3 was slightly excessive and the O_3 conversion dropped to 84% (Fig. 2). In terms of N_2 selectivity, it was high in all three cases and increased from 87% ($C^{in}_{O_3} / C^{in}_{NH_3}$ = 0.85) to 94% ($C^{in}_{O_3} / C^{in}_{NH_3}$ = 1.73), which indicates that higher $C^{in}_{O_3} / C^{in}_{NH_3}$ ratio promotes selective oxidation of NH_3 to N_2 during OZCO process. When the $C^{in}_{O_3} / C^{in}_{NH_3}$ ratio was 1.73, the NH_3 conversion and N_2 selectivity were as high as 99% and 94%, respectively, over AgMn/HZ catalyst at room temperature and GHSV of 150,000 $ml \cdot g^{-1} \cdot h^{-1}$.

3.1.3. Studies on the surface species after OZCO of gaseous NH_3

Fig. 3 shows the ATR spectra of the fresh samples and the used catalysts after OZCO of gaseous NH_3 for 90 min. Compared with the fresh samples (Fig. 3a), new

bands at 1328 cm^{-1}, 1432 cm^{-1}, 3080 cm^{-1} and 3254 cm^{-1} were observed on all used samples (Fig. 3b), which indicates the formation of new species after NH_3 oxidation. Nitrates are one of the frequently recognized intermediates or by-products that would be formed in NH_3 oxidation process.[46,47] But the assignment of these new bands is not straightforward, since the characteristic vibrations are different in literature due to different catalyst preparation and reaction conditions; especially for the high-frequency regions (above 3000 cm^{-1}), the assignments are rare. In order to facilitate the assignment of the new bands on the used catalysts, the spectrum of the NH_4NO_3-HZ, prepared by impregnation of HZ with NH_4NO_3, was also given in Fig. 3b for reference. The same bands as those on the used samples were also observed on the NH_4NO_3-HZ sample. Hence, bands at 1328 cm^{-1} and 1432 cm^{-1} could be assigned to the symmetric and asymmetric stretching vibration of N=O in monodentate nitrates,[48] respectively; bands at 3080 cm^{-1} and 3254 cm^{-1} are attributed to the symmetric and asymmetric stretching of N-H,[49] respectively. Therefore, it is reasonable to deduce that monodentate nitrates and adsorbed ammonia ($[NH_3]_a$) were deposited on the used catalyst surfaces after OZCO of gaseous NH_3.

Moreover, TPD studies were also performed over the used catalysts to further confirm the nature of the surface species after OZCO of gaseous NH_3. Fig. 4 shows the TPD results of the used HZ, Ag/HZ, Mn/HZ and AgMn/HZ catalysts after 90-min OZCO of gaseous NH_3. The desorption of NH_3 was detected on all samples (Fig. S2) and no NO was detected by the FT-IR spectrometer. The MS data are shown in Fig. S3. As shown in Figs. S3a and S3b, no N_2 was formed over HZ and Ag/HZ catalysts.

Figs. 4a and 4b clearly indicate N_2O as the main product over HZ and Ag/HZ catalysts (at 203 ℃ and 202 ℃ for HZ and Ag/HZ catalysts, respectively), together with negligible amount of NO_2. Based on the results of Colombo *et al.*[50] and the ATR results of the used catalysts (Fig. 3b), it is tentatively deduced that N_2O came from the decomposition of ammonia-nitrates complex.[50] H_2O was not produced on HZ and Ag/HZ catalysts, as shown in Fig. 4e. However, besides the evolution of N_2O, N_2 was detected by the mass spectrometer (Figs. S3c and S3d) in a considerable amount at 208 ℃ and 213 ℃ over Mn/HZ and AgMn/HZ catalysts, respectively (Figs. 4c and 4d). Colombo *et al.*[50] also proposed that surface nitrate species ($[\text{-}NO_3]_s$) could be reduced by $[NH_3]_a$ to produce N_2. Hence, it is deduced that N_2 came from the reduction of monodentate nitrates by $[NH_3]_a$ over Mn/HZ and AgMn/HZ catalysts. However, during TPD process, N_2 was not formed on the used HZ and Ag/HZ catalysts, which indicates that MnO_x is necessary for the selective catalytic reduction of $[\text{-}NO_3]_s$ by $[NH_3]_a$ to N_2. Additionally, considerable amount of H_2O was also detected over Mn/HZ and AgMn/HZ catalysts at 218 ℃, as shown in Fig. 4e, which is almost at the same temperature as the evolution of N_2 (at 208 ℃ and 213 ℃ for Mn/HZ and AgMn/HZ catalysts, respectively, as shown in Figs. 4c and 4d) and is attributed as the co-product of the reduction of $[\text{-}NO_3]_s$ by $[NH_3]_a$ to N_2.

3.2. OZCO of adsorbed NH_3

In order to explore the reaction mechanisms for OZCO of gaseous NH_3, OZCO of adsorbed NH_3 was then comparatively performed over HZ, Ag/HZ, Mn/HZ and AgMn/HZ catalysts at room temperature. The surface adsorption sites on the catalysts

towards NH_3 were first investigated by NH_3-TPD technique.

3.2.1 NH_3-TPD results

Fig. 5 shows the NH_3 profiles of HZ, Ag/HZ, Mn/HZ and AgMn/HZ catalysts during NH_3-TPD measurements. Over the HZ support, three NH_3 desorption peaks could be resolved, centered at 116, 161 and 345 ^oC, respectively, as displayed in Fig. 5a. It is commonly recognized that there are three types of NH_3 adsorption sites over H-form zeolite. Brønsted acid (B-acid) sites are formed by the so-called "bridging hydroxyl", which connects the aluminum and silicon atoms in the framework of zeolite;[51] Lewis acid (L-acid) sites are usually composed of aluminum species with low coordination;[51] hydrogen-bonded-physisorption (H-bond) sites are formed by the preceding adsorption of NH_3 on the B-acid sites and this type of sites is non-acidic.[52] Ma *et al.*[53] have assigned the peak at 150 ^oC to the H-bonded NH_3, the peak at 223 ^oC to NH_3 adsorbed on acid sites (L- and B- acid sites) and the peak at 428 ^oC to NH_3 strongly adsorbed on B-acid sites. Similar assignments were also reported by Wang *et al.*,[54] in which it is demonstrated that the NH_3 desorption peaks at 150, 250 and 385 ^oC are due to weakly adsorbed NH_3, NH_3 adsorbed on L-acid sites and B-acid sites, respectively. Additionally, two NH_3 desorption peaks were observed by Al-Dughaither and co-authors[55] and it is indicated that the nature of the weak site was a mixture of L-acid and H-bond sites while the strong site is of predominantly of B-acid sites. According to these results, in this study, the desorption peak at 116 ^oC is assigned to NH_3 on H-bond sites and the peaks at 161 ℃ and 345 ^oC corresponded to the desorption of NH_3 on L-acid and B-acid sites, respectively. Compared with the bare

HZ support, the loading of Ag or (and) MnO_x created new adsorption sites for NH_3. Besides NH_3 desorption from the HZ support (desorption peaks at 116, 181 and 355 ^oC, respectively), a new peak at 445 ^oC was observed on Ag/HZ catalyst, as shown in Fig. 5b, which is due to NH_3 adsorbed on Ag sites. For the Mn/HZ catalyst (Fig. 5c), the NH_3 peak at 260 ^oC is attributed to the desorption of NH_3 adsorbed on MnO_x. Based on the results of Ag/HZ and Mn/HZ catalysts, it can be seen that the addition of Ag caused an even stronger interaction with NH_3 than MnO_x did. As revealed in Fig. 5d, the NH_3 adsorbed on Ag and MnO_x sites over AgMn/HZ catalyst desorbed at 447 ^oC and 215 ^oC, respectively.

3.2.2 OZCO of adsorbed NH_3 and studies on the surface species after OZCO

Fig. 6a exhibits the variations of N_2O and N_2 concentrations with TOS during OZCO of adsorbed NH_3 on HZ, Ag/HZ, Mn/HZ and AgMn/HZ catalysts. It should be noted that, except for N_2O and N_2, no other gaseous products were detected over the four catalysts. From Fig. 6a, it can be seen that N_2O was detected in a noticeable amount with respect to N_2 in gaseous products over HZ and Ag/HZ catalysts and the $N_2O / (N_2 + N_2O)$ ratios are 43% and 38% for HZ and Ag/HZ catalysts, respectively. It can also be seen from Fig. 6a that more N_2 and N_2O were detected over Ag/HZ than HZ, which indicates that the addition of Ag enhanced the OZCO reaction of adsorbed NH_3. However, only small amount of N_2O was detected and no N_2 was formed over Mn/HZ and AgMn/HZ catalysts during OZCO of adsorbed NH_3.

Time course for O_3 conversion during OZCO of adsorbed NH_3 is shown in Fig. 6b. On HZ and Ag/HZ catalysts, O_3 conversion decreased quickly and finally

maintained around 10% and 30%, respectively. On Mn/HZ and AgMn/HZ catalysts, O_3 conversion remained high, but gradual decrease was observed after 20-min and 13-min TOS, respectively. Again, MnO_x is necessary to maintain high and consistent conversion of O_3 in OZCO processes.

In addition, ATR and TPD techniques were also adopted to characterize the surface species after OZCO of adsorbed NH_3.

In order to clearly reflect the changes taking place on the catalyst surface after OZCO of adsorbed NH_3, ATR spectra of fresh samples after adsorption of NH_3 are shown in Fig. 7a. A new band at 1459 cm^{-1} was observed with respect to the fresh samples (Fig. 3a), which is attributed to the bending vibration of NH_4^+ indicating adsorbed NH_3 on B-acid sites.[7,53,54] After OZCO of adsorbed NH_3, the band attributed to NH_3 adsorbed on B-acid sites disappeared, which implies the oxidation of adsorbed NH_3 by O_3, and new bands at 1443 cm^{-1}, 3100 cm^{-1} and 3219 cm^{-1} appeared (Fig. 7b). According to the assignments in **Section 3.1.3**, bands at 3100 cm^{-1} and 3219 cm^{-1} are due to the symmetric and asymmetric stretching of N-H,[49] respectively. Moreover, Hadjiivanov[48] reported that the stretching vibration of N=O in nitrates also occurred at 1380 cm^{-1}. Therefore, the band at 1443 cm^{-1} is assigned to the stretching vibration of N=O of $[\text{-}NO_3]_s$. Therefore, $[\text{-}NO_3]_s$ and $[NH_3]_a$ were deposited on the used catalyst surfaces after OZCO of adsorbed NH_3.

During TPD measurements, the evolution of NH_3 was detected only on HZ and Ag/HZ catalysts, but not on Mn/HZ and AgMn/HZ as shown in Fig. S4. N_2O was detected as main product (at 210 ℃ and 246 ℃ for HZ and Ag/HZ catalysts,

respectively) with negligible amount of NO_2 over HZ and Ag/HZ catalysts during TPD measurements, as shown in Figs. 8a and 8b, respectively, and N_2 was not detected on either of these two samples, as shown in Figs. S5a and S5b. Similar to the TPD measurements after OZCO of gaseous NH_3, N_2O could also come from the decomposition of ammonia-nitrates complex.[50] H_2O was not produced on HZ and Ag/HZ catalysts, as shown in Fig. 8e, which might be due to its low concentration. However, in the cases of Mn/HZ and AgMn/HZ catalysts, N_2 was detected by the mass spectrometer (Figs. S5c and S5d) at 201 ℃ and 211 ℃, respectively, and in a considerable amount (Figs. 8c and 8d) during TPD measurements, which came from the reduction of $[\text{-}NO_3]_s$ by $[NH_3]_a$.[50] N_2O was also formed on Mn/HZ and AgMn/HZ catalysts, as shown in Figs. 8c and 8d, which was derived from the decomposition of ammonia-nitrates complex. Large amount of H_2O was also detected over Mn/HZ and AgMn/HZ catalysts at 250 ℃, as shown in Fig. 8e and is attributed to the decomposition of ammonia-nitrates complex and the reduction of $[\text{-}NO_3]_s$ by $[NH_3]_a$. No NH_3 was evolved over Mn/HZ and AgMn/HZ catalysts (Fig. S4) during TPD measurements since all the residual NH_3 after OZCO of adsorbed NH_3 reacted with nitrates in TPD processes.

3.3. Proposed reaction pathways for OZCO of gaseous NH_3

In the cases of HZ and Ag/HZ catalysts, the same gaseous products (N_2O and N_2) as those of OZCO of gaseous NH_3 (Fig. 1c) were also detected during OZCO of adsorbed NH_3, as shown in Fig. 6a. Although the $N_2O/(N_2+N_2O)$ ratios were 43% and 38% for HZ and Ag/HZ catalysts, respectively, which are higher than those of

OZCO of gaseous NH_3 (The N_2O selectivities were less than 10% over HZ and Ag/HZ catalysts, as shown in Fig. 1c), N_2 was still the main product during OZCO of adsorbed NH_3. The reasonable explanation to the higher ratios of $N_2O/(N_2+N_2O)$ during OZCO of adsorbed NH_3 is as follows: during OZCO of adsorbed NH_3, O_3 was continuously fed into catalyst bed after NH_3 adsorption. Therefore, O species, including O_3(g) and adsorbed atomic oxygen $[O^*]_a$, were excessive with respect to the decreasing amount of adsorbed NH_3. As a result, the adsorbed NH_3 was more likely to be further oxidized by O species to produce N_2O in contrast to OZCO of gaseous NH_3.

In addition, as shown in Fig. 6b, O_3 conversion during OZCO of adsorbed NH_3 also exhibited similar stability as that of OZCO of gaseous NH_3 (Fig. 1b). O_3 conversions of HZ and Ag/HZ catalysts were comparable to those of Mn/HZ and AgMn/HZ catalysts in the initial several minutes due to O_3 consumption by the pre-adsorbed NH_3 and thereafter stabilized at around 10% and 30% (Fig. 6b), respectively. These values of the O_3 conversion were much lower than those in OZCO of gaseous NH_3 (60% and 80% for HZ and Ag/HZ, respectively, as shown in Fig. 1b), which can be ascribed to that HZ and Ag/HZ are intrinsically less active for O_3 decomposition in the absence of NH_3.

Moreover, the surface species on the used HZ and Ag/HZ catalysts after OZCO of gaseous and adsorbed NH_3 were all composed of $[\text{-}NO_3]_s$ and $[NH_3]_a$, as indicated by the ATR characterization in Figs. 3b and 7b. TPD results of the used catalysts after OZCO of adsorbed NH_3 were also very similar to those after OZCO of gaseous NH_3:

only NH_3 and N_2O were detected, besides the negligible amount of NO_2, and no N_2 was observed. Based on the similarities of ATR and TPD results of the used catalysts between OZCO of gaseous and adsorbed NH_3 and the low activity of HZ and Ag/HZ catalysts in O_3 decomposition, it is reasonable to deduce that OZCO of gaseous NH_3 over HZ and Ag/HZ catalysts proceeds through Pathway (A) in Fig. 9, which means that NH_3(g) is first adsorbed on the catalyst surface to form $[NH_3]_a$ and then the $[NH_3]_a$ is oxidized by O species to final product N_2. Besides $[NH_3]_a$ oxidation in Pathway (A), O_3 could also be consumed via catalytic decomposition (Pathway (C) in Fig. 9) over HZ and Ag/HZ catalysts.

On the other hand, for Mn/HZ and AgMn/HZ catalysts, gaseous products were barely detected during OZCO of adsorbed NH_3 (Fig. 6a), which is totally different from the result of OZCO of gaseous NH_3 (N_2 was detected as the major gaseous product during OZCO of gaseous NH_3, as shown in Fig. 1c). In addition, O_3 conversion also showed different stability in OZCO of gaseous (Fig. 1b) and adsorbed (Fig. 6b) NH_3. It could be attributed to the fast accumulation of nitrates on the surface of Mn/HZ and AgMn/HZ catalysts during OZCO of adsorbed NH_3, which would occupy the active sites for O_3 decomposition. Moreover, the surface species accumulated on the catalyst surface after OZCO of adsorbed NH_3 were different from those after OZCO of gaseous NH_3, which can be deduced from the huge difference in the ratios of N_2 to N_2O formed in TPD measurements after OZCO processes (The ratios of N_2 to N_2O were 1 for the former case (Figs. 8c and 8d) and 8 for the latter case (Figs. 4c and 4d)). Based on the differences between OZCO of gaseous and

adsorbed NH_3 and the high activity of Mn/HZ and AgMn/HZ catalysts in O_3 decomposition, it is reasonable to deduce that OZCO of gaseous NH_3 over Mn/HZ and AgMn/HZ catalysts proceeds through Pathway (B) in Fig. 9, in which O_3(g) is first catalytically decomposed to form adsorbed atomic oxygen $[O^*]_a$ on the catalyst surface and then the NH_x species are oxidized by $[O^*]_a$ to final product N_2.

Based on the proposed reaction mechanism, the results of OZCO of gaseous NH_3 in Fig. 1 could be explained as follows. For HZ and Ag/HZ catalysts, the NH_3 adsorption rate is much higher than the $[NH_3]_a$ oxidation rate by O species in Pathway (A) , so the latter is the rate-controlling step in OZCO of gaseous NH_3 over HZ and Ag/HZ catalysts. However, as the reaction proceeded, more active sites on HZ and Ag/HZ catalysts would be occupied by $[NH_3]_a$ resulting in the decrease in NH_3 conversion with TOS, as shown in Fig. 1a. In addition, O_3 could be consumed through both Pathways (A) and (C) over HZ and Ag/HZ catalysts. At the initial stage of the OZCO reaction, O_3 was consumed mainly by Pathway (A) due to the large amount of active sites on the catalyst surface. However, as the reaction went on, Pathway (A) was gradually inhibited by the adsorbed NH_3 molecules, so Pathway (C) became the main path responsible for O_3 consumption. Therefore, the O_3 conversion remained almost constant in general with TOS over HZ and Ag/HZ catalysts during OZCO of gaseous NH_3, as shown in Fig. 1b. This is also supported by the $n_{O_3}^{Conv.}/n_{NH_3}^{Conv.}$ ratios of the reactions. As shown in Fig 1d, the initial $n_{O_3}^{Conv.}/n_{NH_3}^{Conv.}$ ratios of reactions over HZ and Ag/HZ were around 1.4 and 1.3, respectively, which are lower than the stoichiometric ratio of 1.5 in eqn. (8). This is likely due to the fact that more than one

oxygen atoms per O_3 molecule are involved in NH_3 oxidation to N_2 in Pathway (A). As the OZCO reaction went on, the $n_{O_3}^{Conv.}/n_{NH_3}^{Conv.}$ ratios of HZ and Ag/HZ catalysts increased and were more than the stoichiometric ratio of 1.5 (Fig. 1d) in eqn. (8), which indicates that Pathway (C) had become the main route for O_3 consumption over HZ and Ag/HZ catalysts.

However, for Mn/HZ and AgMn/HZ catalysts, since the O_3 decomposition and NH_3(g) oxidation by $[O^*]_a$ are both at high reaction rate, NH_3 and O_3 conversions were almost constant during OZCO of gaseous NH_3 over Mn/HZ and AgMn/HZ, as shown in Figs. 1a and 1b, respectively. Based on the two parallel reactions in eqns. (8) and (9), it is possible to calculate the theoretical $n_{O_3}^{Conv.}/n_{NH_3}^{Conv.}$ ratio of the reaction according to N_2O and N_2 selectivities. Since the selectivities of N_2O & N_2 were 20% & 80% and 13% & 87% for Mn/HZ and AgMn/HZ catalysts (Fig. 1c), respectively, the theoretical $n_{O_3}^{Conv.}/n_{NH_3}^{Conv.}$ ratios can be calculated ($1.5\times S_{N_2}+2\times S_{N_2O}$) to be about 1.60 and 1.57 for Mn/HZ and AgMn/HZ, respectively, which are consistent with the experimental results, ~1.7 for Mn/HZ and ~1.65 for AgMn/HZ.

There also exists another possible mechanism where the reaction pathway might be the same over the four catalysts but the reaction rates of Mn/HZ and AgMn/HZ catalysts are much faster than those of HZ and Ag/HZ catalysts, which results from the high ability of Mn/HZ and AgMn/HZ catalysts to activate ozone. The mechanism will be further studied in the future work.

Conclusions

OZCO for removing ammonia from simulated air at room temperature was studied in this paper. Compared with HZ, Ag/HZ and Mn/HZ catalysts, AgMn/HZ catalyst exhibited high activity, good stability and high N_2 selectivity, which could be attributed to the outstanding ability of MnO_x to decompose O_3 and the promoting effect of Ag. The NH_3 conversion and N_2 selectivity were as high as 99% and 94%, respectively, over AgMn/HZ catalyst at room temperature, GHSV of 150,000 $ml \cdot g^{-1} \cdot h^{-1}$ and $C^{in}_{O_3}/C^{in}_{NH_3}$ ratio of 1.73 that is slightly higher than the stoichiometric ratio of OZCO of NH_3 to N_2. The possible pathway for OZCO of NH_3 over AgMn/HZ catalyst was proposed as follows: $O_3(g)$ is first adsorbed and decomposed into $[O^*]_a$ and then NH_x species are oxidized by $[O^*]_a$ to form N_2. This was supported by the results of comparison between OZCO of adsorbed and gaseous NH_3.

Acknowledgements

This work is supported by National Natural Science Foundation of China (11079013, U1201231) and by the Welch Foundation in US (#T-0014).

‡Notes

1 GHSV (Gas Hourly Space Velocity) represents the amount of gas mixture flowing over catalysts per unit gram of catalyst per unit time and can be calculated by the following equation:

$$\mathrm{GHSV} = \frac{F}{m_{\mathrm{cat}}}$$

where F and m_{cat} represent the total volume flow rate of reaction gas and mass of

catalyst, respectively.

2 BET surface area is calculated using the theory of adsorption of polymolecular layer defined by Brunauer, Emmett and Teller.

3 SCCM is an abbreviation of Standard Cubic Centimeters per Minute indicating $ml \cdot min^{-1}$ at a standard temperature of zero ^{o}C and pressure of 101.325 kPa.

References

1 J.R. Kastner, J. Miller, P. Kolar and K.C. Das, *Chemosphere*, 2009, **75**, 739.
2 Y. Li and J.N. Armor, *Appl. Catal. B: Environ.*, 1997, **13**, 131.
3 L. Lietti, G. Ramis, G. Busca, F. Bregani and P. Forzatti, *Catal. Today*, 2000, **61**, 187.
4 R.Q. Long and R.T. Yang, *J. Catal.*, 2001, **201**, 145.
5 R.Q. Long and R.T. Yang, *J. Catal.*, 2002, **207**, 158.
6 L. Gang, B.G. Anderson, J. van Grondelle and R.A. van Santen, *Appl. Catal. B: Environ.*, 2003, **40**, 101.
7 G. Qi, J.E. Gatt and R.T. Yang, *J. Catal.*, 2004, **226**, 120.
8 L. Chmielarz, P. Kuśtrowski, A. Rafalska-Łasocha and R. Dziembaj, *Appl. Catal. B: Environ.*, 2005, **58**, 235.
9 A.C. Akah, G. Nkeng and A.A. Garforth, *Appl. Catal. B: Environ.*, 2007, **74**, 34.
10 M.J. Lippits, A.C. Gluhoi and B.E. Nieuwenhuys, *Catal. Today*, 2008, **137**, 446.
11 M.S. Kim, D.W. Lee, S.H. Chung, Y.K. Hong, S.H. Lee, S.H. Oh, I.H. Cho and K.Y. Lee, *J. Hazard. Mater.*, 2012, **237-238**, 153.
12 C. Liang, X. Li, Z. Qu, M. Tade and S. Liu, *Appl. Surf. Sci.*, 2012, **258**, 3738.
13 A. Naydenov and D. Mehandjiev, *Appl. Catal. A: Gen.*, 1993, **97**, 17.
14 D. Mehandjiev, K. Cheshkova, A. Naydenov and V. Georgesku, *Reac. Kinet. Catal. Lett.*, 2002, **76**, 287.
15 S. Dimitrova, G. Ivanov and D. Mehandjiev, *Appl. Catal. A: Gen.*, 2004, **266**, 81.
16 P. Konova, M. Stoyanova, A. Naydenov, St. Christoskova and D. Mehandjiev, *Appl. Catal. A: Gen.*, 2006, **298**, 109.
17 H. Einaga and S. Futamura, *J. Catal.*, 2004, **227**, 304.
18 H. Einaga and A. Ogata, *J. Hazard. Mater.*, 2009, **164**, 1236.
19 H. Einaga and A. Ogata, *Environ. Sci. Technol.*, 2010, **44**, 2612.
20 H. Einaga, N. Maeda and Y. Teraoka, *Appl. Catal. B: Environ.*, 2013, **142-143**, 406.
21 H. Einaga, Y. Teraoka and A. Ogata, *J. Catal.*, 2013, **305**, 227.
22 C.R. Lee, J. Jurng, G.N. Bae, J.K. Jeon, S.C. Kim, J.M. Kim, M. Jin and Y.K. Park, *J. Nanosci. Nanotechno.*, 2011, **11**, 7303.
23 J.H. Park, J.M. Kim, M. Jin, J.K. Jeon, S.S. Kim, S.H. Park, S.C. Kim and Y.K. Park, *Nanoscale Res. Lett.*, 2012, **7**, 14.

24 M. Jin, J.W. Kim, J.M. Kim, J. Jurng, G.N. Bae, J.K. Jeon and Y.K. Park, *Powder Technol.*, 2011, **214**, 458.
25 Y. Liu, X.S. Li, C. Shi, J.L. Liu, A.M. Zhu and Ben W.-L. Jang, *Catal. Sci. Technol.*, 2014, **4**, 2589.
26 Y. Liu, X.S. Li, J.L. Liu, C. Shi and A.M. Zhu, *Chin. J. Catal.*, 2014, **35**, 1465.
27 E. Rezaei and J. Soltan, *Chem. Eng. J.*, 2012, **198-199**, 482.
28 E. Rezaei, J. Soltan, N. Chen and J. Lin, *Chem. Eng. J.*, 2013, **214**, 219.
29 E. Rezaei, J. Soltan and N. Chen, *Appl. Catal. B: Environ.*, 2013, **136-137**, 239.
30 C.Y.H. Chao, C.W. Kwong and K.S. Hui, *J. Hazard. Mater.*, 2007, **143**, 118.
31 M. Li, K.N. Hui, K.S. Hui, S.K. Lee, Y.R. Cho, H. Lee, W. Zhou, S. Cho, C.Y.H. Chao and Y. Li, *Appl. Catal. B: Environ.*, 2011, **107**, 245.
32 E. Park, S. Chin, J. Kim, G.N. Bae and J. Jurng, *Powder Technol.*, 2011, **208**, 740.
33 H.H. Kim, M. Sugasawa, H. Hirata, Y. Teramoto, K. Kosuge, N. Negishi and A. Ogata, *Plasma Chem. Plasma Process*, 2013, **33**, 1083.
34 H.C. Wang, H.S. Liang and M.B. Chang, *J. Hazard. Mater.*, 2011, **186**, 1781.
35 H.S. Liang, H.C. Wang and M.B. Chang, *Ind. Eng. Chem. Res.*, 2011, **50**, 13322.
36 D.Z. Zhao, T.Y. Ding, X.S. Li, J.L. Liu, C. Shi and A.M. Zhu, *Chin. J. Catal.*, 2012, **33**, 396.
37 D.Z. Zhao, C. Shi, X.S. Li, A.M. Zhu and Ben W.-L. Jang, *J. Hazard. Mater.*, 2012, **239-240**, 362.
38 M. Stoyanova, P. Konova, P. Nikolov, A. Naydenov, St. Christoskova and D. Mehandjiev, *Chem. Eng. J.*, 2006, **122**, 41.
39 Z. Hao, D. Cheng, Y. Guo and Y. Liang, *Appl. Catal. B: Environ.*, 2001, **33**, 217.
40 M. Petersson, D. Jonsson, H. Persson, N. Cruise and B. Andersson, *J. Catal.*, 2006, **238**, 321.
41 S. Ichikawa, L. Mahardiani and Y. Kamiya, *Catal. Today*, 2014, **232**, 192.
42 S.T. Oyama, *Catal. Rev.: Sci. Eng.*, 2000, **42**, 279.
43 K.J. Olszyna and J. Heicklen, in *Photochemical Smog and Ozone Reactions*, ed. R.F. Gould, American Chemical Society, Washington, DC, 1972, vol. 113, ch. 6, pp. 191-210.
44 E.M. Slavinskaya, S.A. Veniaminov, P. Nottét, A.S. Ivanova, A.I. Boronin, Yu.A. Chesalov, I.A. Polukhina and A.S. Noskov, *J. Catal.*, 2004, **222**, 129.
45 W. Li, G.V. Gibbs and S.T. Oyama, *J. Am. Chem. Soc.*, 1998, **120**, 9041.
46 A. Savara, W.M.H. Sachtler and E. Weitz, *Appl. Catal. B: Environ.*, 2009, **90**, 120.
47 S. Tamm, N. Vallim, M. Skoglundh and L. Olsson, *J. Catal.*, 2013, **307**, 153.
48 K.I. Hadjiivanov, *Catal. Rev.: Sci. Eng.*, 2000, **42**, 71.
49 *The Sadtler Handbooks of Infrared Spectra*, Bio-Rad Laboratories, Inc., Informatics Division.
50 M. Colombo, I. Nova and E. Tronconi, *Catal. Today*, 2012, **197**, 243.
51 L. Rodríguez-González, F. Hermes, M. Bertmer, E. Rodríguez-Castellón, A. Jiménez-López and U. Simon, *Appl. Catal. A: Gen.*, 2007, **328**, 174.
52 N. Katada and M. Niwa, *Cataly. Surv. Asia*, 2004, **8**, 161.
53 L. Ma, Y. Cheng, G. Cavataio, R.W. McCabe, L. Fu and J. Li, *Appl. Catal. B: Environ.*, 2014, **156-157**, 428.
54 D. Wang, L. Zhang, J. Li, K. Kamasamudram and W.S. Epling, *Catal. Today*, 2014, **231**, 64.
55 A.S. Al-Dughaither and H. de Lasa, *Ind. Eng. Chem. Res.*, 2014, **53**, 15303.

Figure Captions

Fig. 1. Time courses for (a) NH_3 conversion, (b) O_3 conversion, (c) N_2O and N_2 selectivities and (d) $n_{O_3}^{Conv.}/n_{NH_3}^{Conv.}$ ratio during OZCO of gaseous NH_3 over HZ, Mn/HZ, Ag/HZ and AgMn/HZ catalysts. Conditions: 0.1 g of catalysts, feed gas of 250 SCCM containing 530 ppmv of NH_3, 450 ppmv of O_3, 20 vol.% of O_2 and balanced by N_2.

Fig. 2. Effects of $C_{O_3}^{in}/C_{NH_3}^{in}$ ratio on OZCO of gaseous NH_3 over AgMn/HZ catalyst at TOS = 60 min. Conditions: 0.1 g of AgMn/HZ catalyst, 250 SCCM of flow rate with 530 ppmv ($C_{O_3}^{in}/C_{NH_3}^{in}=0.85$), 517 ppmv ($C_{O_3}^{in}/C_{NH_3}^{in}=1.32$) and 521 ppmv ($C_{O_3}^{in}/C_{NH_3}^{in}=1.73$) of NH_3, respectively, in 20 vol.% O_2 / 80 vol.% N_2.

Fig. 3. ATR spectra of the catalysts: (a) fresh samples and (b) used catalysts after OZCO of gaseous NH_3 for 90 min. OZCO conditions are the same as those in **Fig. 1**. NH_4NO_3-impregnated HZ (NH_4NO_3-HZ) was prepared for reference. Preparation of the NH_4NO_3-HZ sample involves impregnation of HZ with NH_4NO_3 solution and then drying at 50 ℃ for 12 h.

Fig. 4. TPD profiles of the used catalysts after 90-min OZCO of gaseous NH_3: the concentrations of N_2O and NO_2 on (a) HZ and (b) Ag/HZ catalysts; the concentrations of N_2, N_2O and NO_2 on (c) Mn/HZ and (d) AgMn/HZ catalysts; (e) the strongest FT-IR peak height of water in the range of 3500 to 4000 cm^{-1}. OZCO conditions are the same as those in **Fig. 1**. TPD conditions: 0.03 g of the used catalysts, 100 SCCM of He, 10 ℃·min^{-1}.

Fig. 5. NH_3 profiles of (a) HZ, (b) Ag/HZ, (c) Mn/HZ and (d) AgMn/HZ catalysts

during NH_3-TPD measurements. NH_3 adsorption conditions: 0.1 g of catalysts, 540 ppmv of NH_3 for 25-min adsorption; TPD conditions: 100 SCCM of Ar, 10 ℃·min^{-1}.

Fig. 6. Time courses for (a) N_2O and N_2 concentrations and (b) O_3 conversion during OZCO of adsorbed NH_3 over HZ, Mn/HZ, Ag/HZ and AgMn/HZ catalysts. NH_3 adsorption conditions: 0.1 g of catalysts, 540 ppmv of NH_3 for 25-min adsorption; OZCO conditions: a feed gas of 250 SCCM containing 450 ppmv of O_3, 20 vol.% of O_2 and balanced by He.

Fig. 7. ATR spectra of the catalysts (a) after their exposure to certain amount of NH_3 and (b) after 30-min OZCO of adsorbed NH_3. NH_3 adsorption and OZCO conditions are the same as those in **Fig. 6.**

Fig. 8. TPD profiles of the used catalysts after 30-min OZCO of adsorbed NH_3: the concentrations of N_2O and NO_2 on (a) HZ and (b) Ag/HZ catalysts; the concentrations of N_2, N_2O and NO_2 on (c) Mn/HZ and (d) AgMn/HZ catalysts; (e) the strongest FT-IR peak height of water in the range of 3500 to 4000 cm^{-1}. OZCO conditions are the same as those in **Fig. 6**. TPD conditions: 0.03 g of the used catalysts, 100 SCCM of He, 10 ℃·min^{-1}.

Fig. 9. Proposed reaction pathways for OZCO of gaseous NH_3 over HZ, Ag/HZ, Mn/HZ and AgMn/HZ catalysts.

Fig. 1

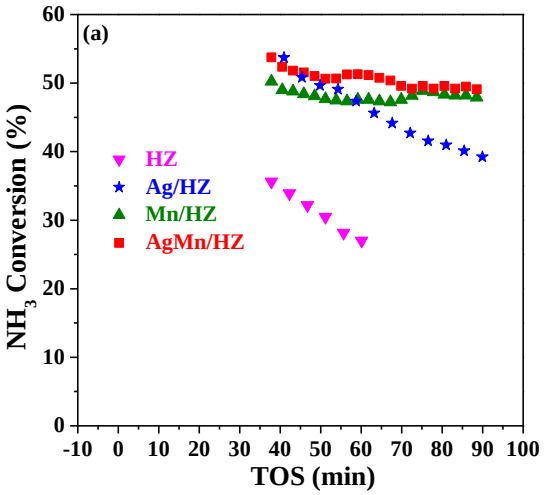

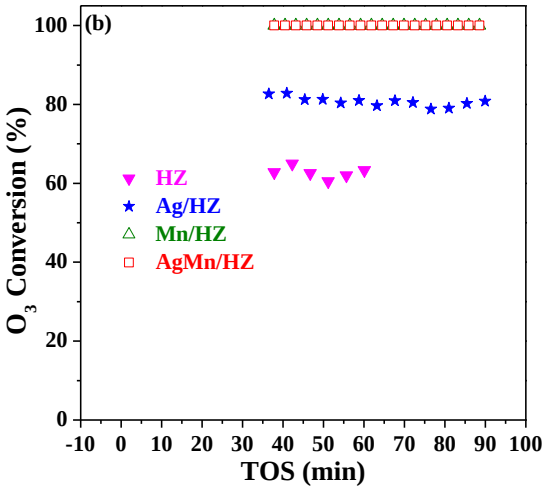

Fig. 1

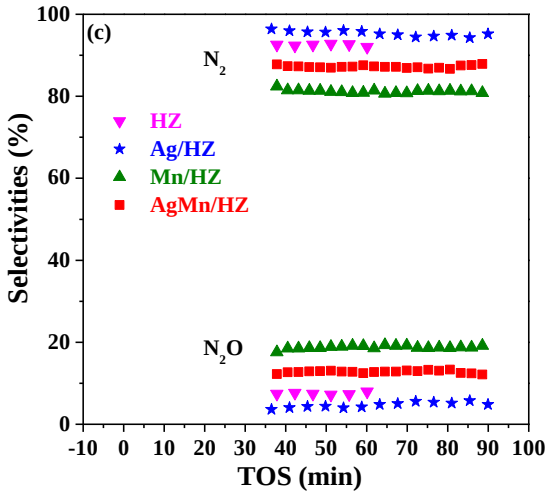

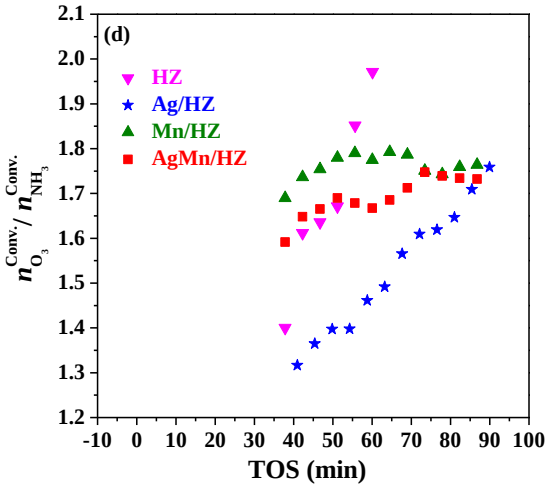

Fig. 2

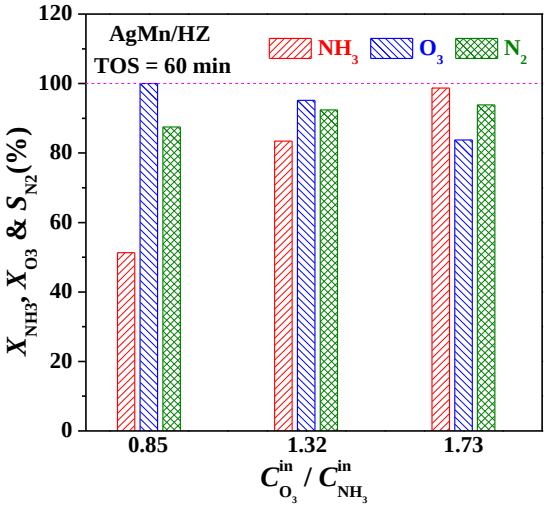

Fig. 3

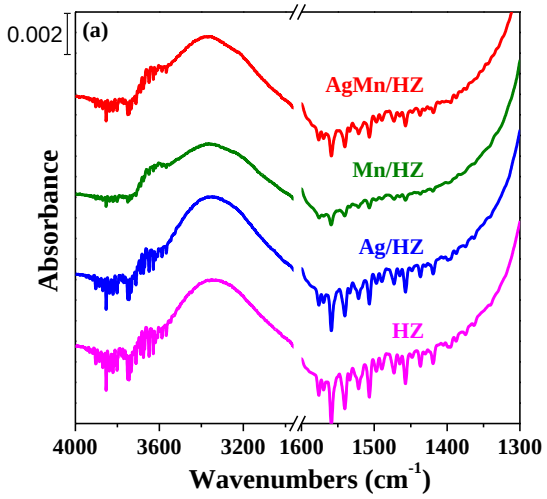

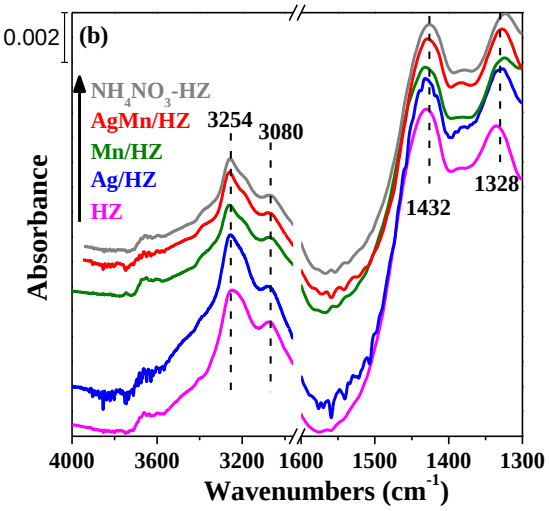

Fig. 4

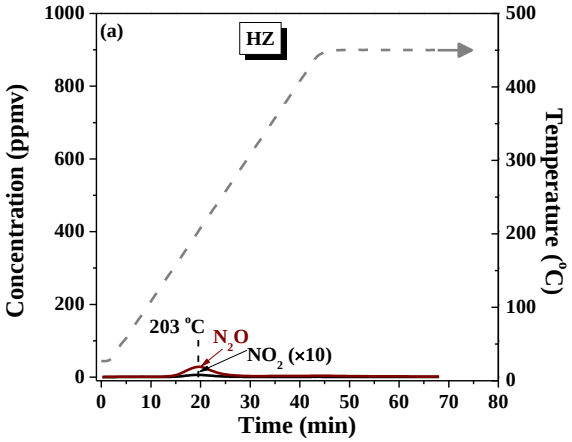

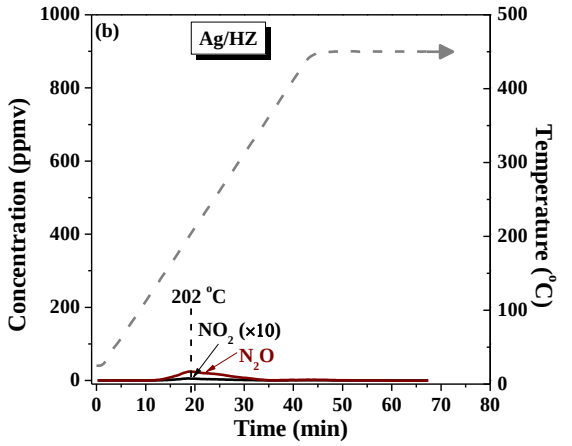

Fig. 4

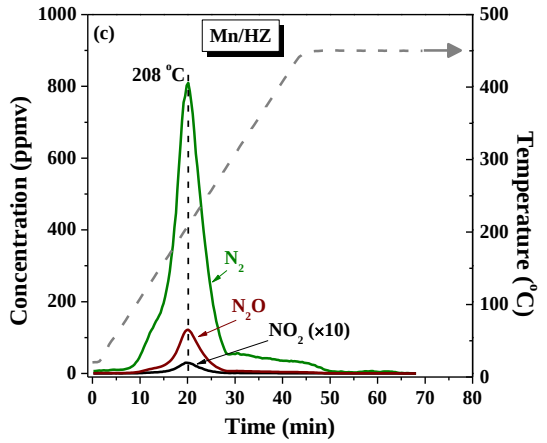

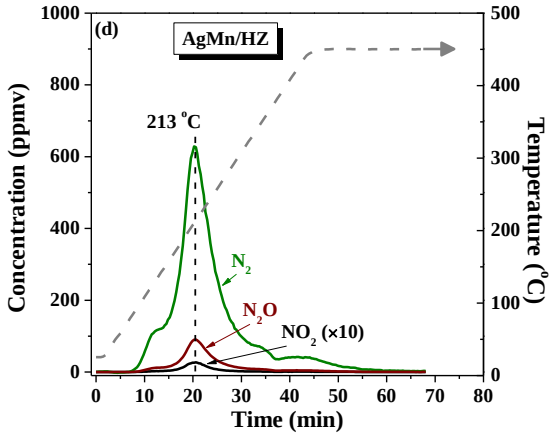

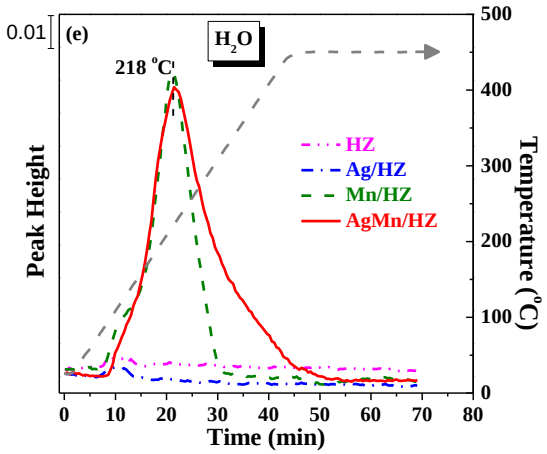

Fig. 5

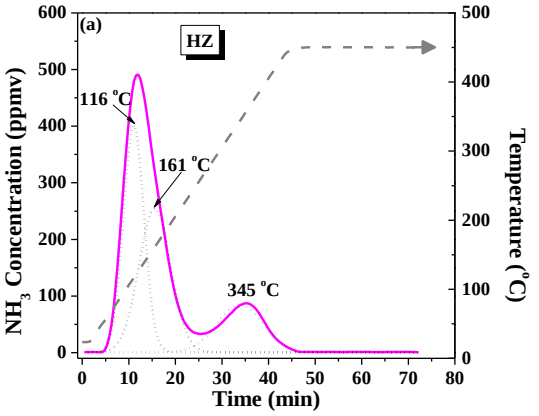

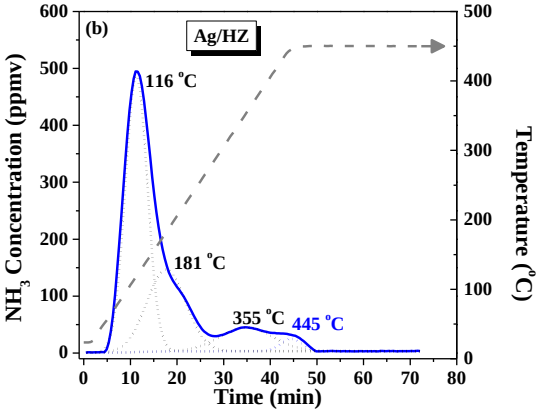

Fig. 5

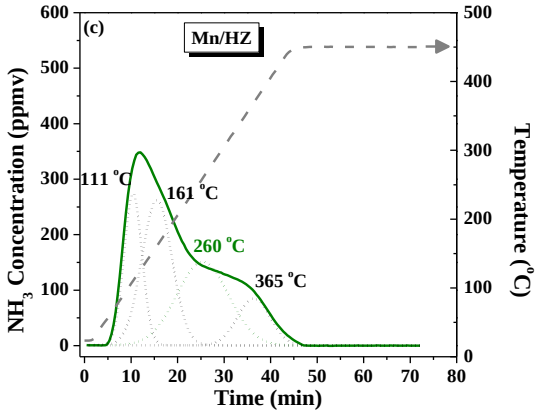

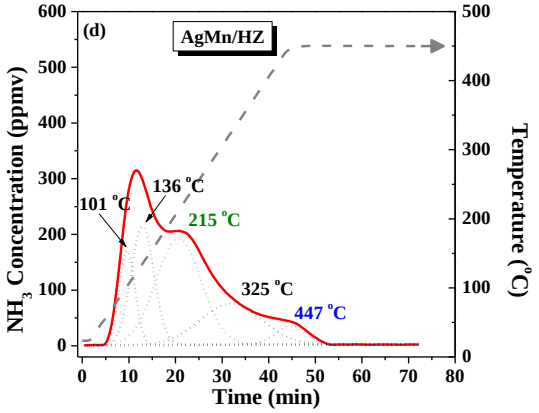

Fig. 6

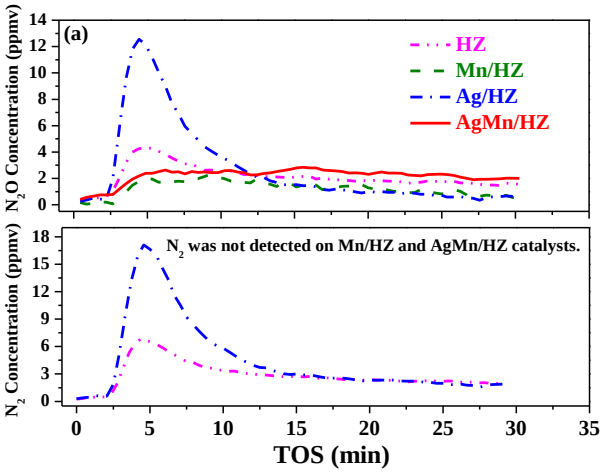

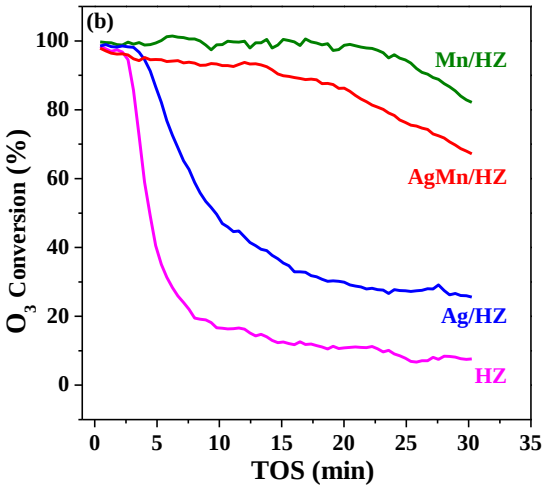

Fig. 7

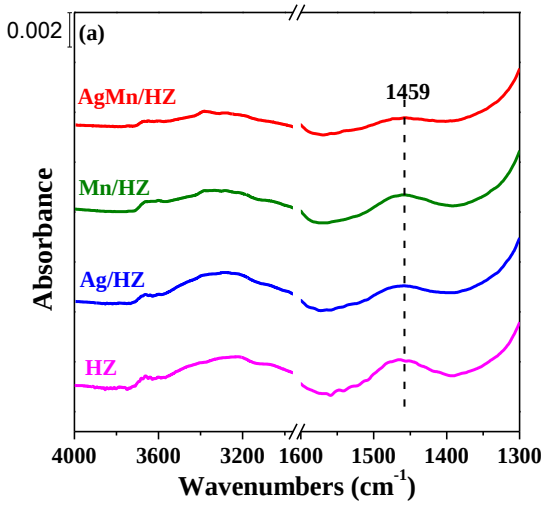

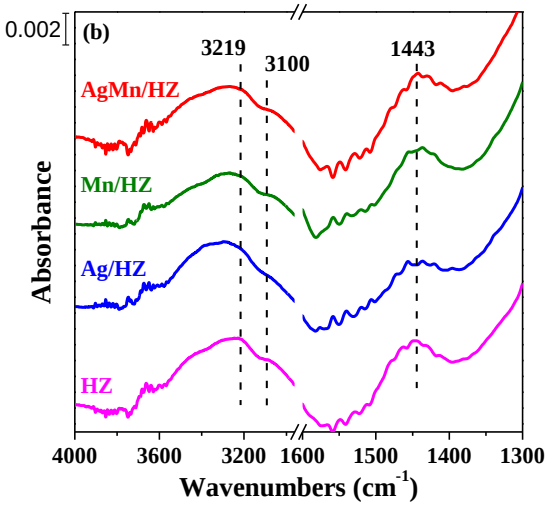

Fig. 8

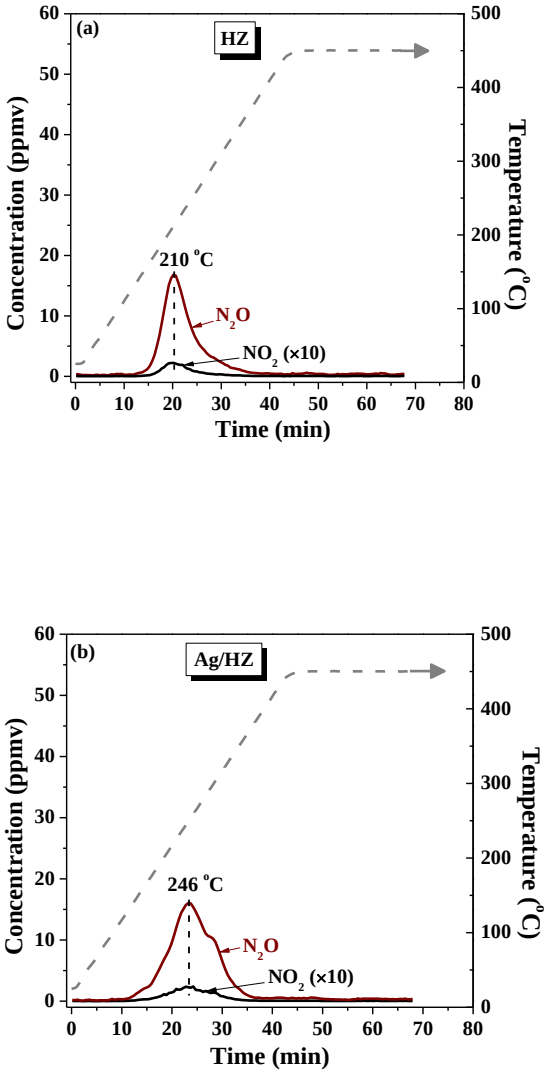

Fig. 8

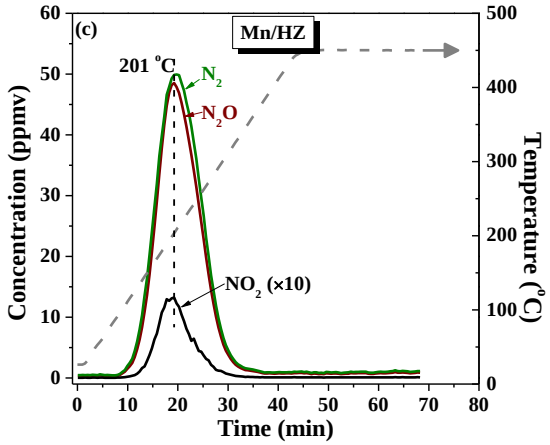

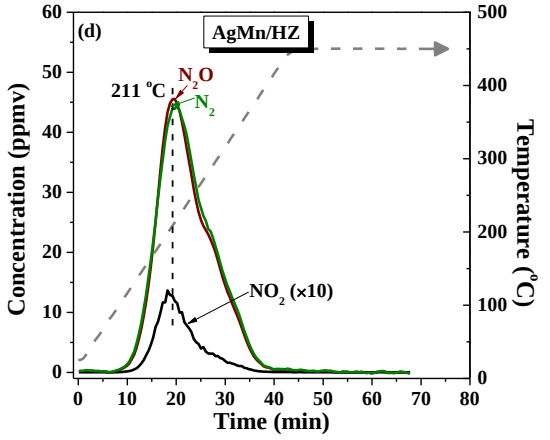

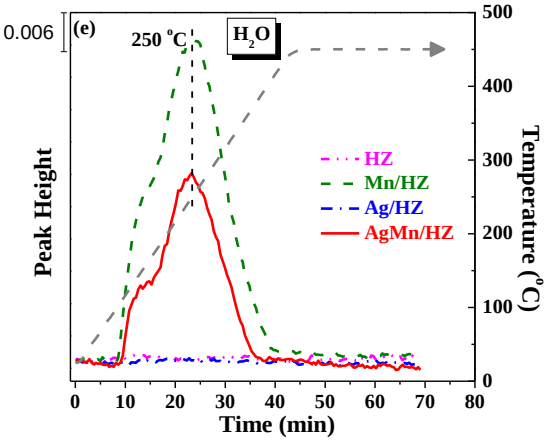

Fig. 9